IEEE Access
Multidisciplinary | Rapid Review | Open Access Journal

Received December 6, 2021, accepted February 13, 2022, date of publication February 17, 2022, date of current version March 2, 2022.

Digital Object Identifier 10.1109/ACCESS.2022.3152605

Secrecy Capacity of Diffusive Molecular Communication Under Different Deployments

S. PRATAP SINGH[1], (Member, IEEE), SUMAN YADAV[2], RAJNEESH KUMAR SINGH[3], VINEET KANSAL[4], AND GHANSHYAM SINGH[5]

[1]Department of Electronics and Communication Engineering, Galgotias College of Engineering and Technology, Greater Noida, Uttar Pradesh 201306, India
[2]Department of Electronics and Communication Engineering, Lloyd Institute of Engineering and Technology, Greater Noida, Uttar Pradesh 201306, India
[3]Department of Computer Applications, Galgotias College of Engineering and Technology, Greater Noida, Uttar Pradesh 201306, India
[4]Department of Computer Science and Engineering, Institute of Engineering and Technology, Lucknow, Uttar Pradesh 226021, India
[5]Centre for Smart Information and Communication Systems, Department of Electrical and Electronic Engineering Science, Auckland Park Kingsway Campus, University of Johannesburg, Johannesburg 2006, South Africa

Corresponding author: Ghanshyam Singh (ghanshyams@uj.ac.za)

ABSTRACT Currently, the physical layer security is considered as one of the most suitable security techniques in Diffusive Molecular Communication (DMC) because of ease to implement. A recent piece of literature has presented the Secrecy Capacity (SC) of DMC system under the rectangular deployment. To evaluate the information capacity (IC) and thereby SC using the Concentration Greens Function (CGF) in the molecular communication depends on the biological structures of tissues. In this paper, we have investigated the analytical expressions of IC under both the Biological Cylindrical Deployment (BCD) and Biological Spherical Deployment (BSD). Therefore, the analytical expressions of IC have been employed to derive the mathematical expressions of SC under the BCD and BSD environment. Further, the SC is analyzed as a function of distance/radius considering the power and/or bandwidth as the parameter. In addition, the effect of distance of authentic receiver on SC is also explored. It is observed that irrespective of the deployments, the distance of the authentic receiver illustrates predominant effect on the value of SC. The proposed analysis is useful in the implementation of DMC under different tissues structures. The numerically simulated results show close agreement with the theoretical background.

INDEX TERMS Secrecy capacity, biological spherical deployment, biological cylindrical deployment, concentration greens function, molecular communication.

I. INTRODUCTION

In the last decade, various Nanoscale devices have been designed and engineered to facilitate the exchange of information through diffusion in the fluidic biological medium [1] which leads to a new paradigm of modern communication system known as diffusive molecular communication (DMC) that is bio-compatible and energy-efficient. It is important to mention that the DMC in diffusion is a mechanism used for the propagation of information from transmitter to receiver, where molecules are the carriers [2], [3]. Further, it is noteworthy to mention that DMC has profound applications in the field of medical such as in targeted drug delivery, detection and monitoring of disease, and regenerative medicines [4]–[6] among the others. The diffusion in DMC could be bounded or unbounded but the DMC in the unbounded environment has a very limited range of communication which is not appropriate to fulfill the requirements of healthcare applications. However, several researchers have suggested that the DMC over bounded microfluidic channels are suitable for long-range communications due to confining nature of information propagation in a guided manner [7]. These are the following three types of possible bounded microfluidic diffusion channels namely, rectangular, cylindrical, and spherical deployments are proposed in the literature. In the case of the rectangular microfluidic channel, the operational frequencies for communication are limited as an increase in frequency results in a very high attenuation [8]. On the other hand, the bounded cylindrical deployment is a more suitable model for the microfluidic channel [9]. The modeling of the complex shape of blood vessels as cylinders is widely accepted as proposed by Fournier [10] for the design and implementation of a DMC system inside the blood vessels for healthcare applications. Further, the cylindrical deployment with a smaller radius improves the system performance by increasing the strength

The associate editor coordinating the review of this manuscript and approving it for publication was Rui Wang.

of the received signal. Moreover, the biological spherical structure of the human body such as stomach, lungs, kidneys bounded spherical deployment is proposed in [11], which is useful in predicting the drug concentration profile in targeted drug delivery applications. In addition, the authors in [12], [13] have presented DMC in which virus particles have been considered as information carriers. Walsh et. al. [12] have suggested the control of pro viral genes for selection of payload, it's packing, and addressing of viruses in a different cell. However, controlled interaction and degradation of a drug under different biological deployments are explored in [13]. Further, the DMC under drift is presented in [14], [15] for drug delivery via the cardiovascular system in which the blood cell collisions have been included. Further, the authors in [16]–[18] and [19], [20] have employed the DMC system for Oncological and Optogenetics respectively.

As aforementioned, various reported pieces of literature have suggested the use of DMC systems in the detection, monitoring, and treatment of different diseases under different deployments. In sequence, authors in [1], [8], [9], [21]–[28] have considered different deployments in the analytical modeling of the DMC system. In [8], a rectangular micro-fluidic deployment is modeled and analyzed for flow-induced DMC. The structure of particular entities in the body has motivated us to explore the spherical and cylindrical diffusion channels for DMC systems [1], [9], [21]–[25]. Yeh et.al. in [1] have considered a tunnel-like environment without flow for DMC where the receiver partly covers the cross-section of the reflective cylinder. Further, the distribution of hitting locations is computed based on the simulation results, which in fact does not reflect an exact distribution. In [9], the authors have proposed the concentration Green's Function (CGF) in a cylindrical environment with uniform flow. Further, the boundary is covered with receptor proteins and information carriers are affected by both the flow and chemical degradation. However, the impact of a reversible receptor with the reactive receiver also needs to explore. In [21], a cylindrical DMC system is modeled without flow and absorbing walls, whereas in [22] a cylindrical environment in a DMC is presented with reflective receiver and non-uniform fluid flow. Further, the spherical biological structures of the body such as stomach, lungs, kidneys, cells, etc. have motivated us to consider a bounded spherical environment [23]–[25]. Al-Zu'bi and Mohan [23] have considered a DMC system in a bounded spherical environment with completely absorbing walls where the transmitter is a point source and receiver covered with ligand-receptor which is placed at the center of the sphere. However, the authors in [24] have considered a completely reflective wall with the receiver at the center of the spherical deployment. Finally, Bao et.al. [25] have presented a point source transmitter at the center of the boundary and compute the molecule concentration of the DMC system with a fully closed reflective and absorptive spherical boundary.

Due to the presence of eavesdroppers in the network, it is imperative to say that security is the utmost issue for any wireless communication system. Therefore, the physical layer security, being easy to implement, is regarded as one of the most suitable security techniques. Furthermore, the secrecy capacity (SC) is the most important parameter in the implementation of physical layer security of any communication system however, it depends on the information capacity (IC). Again, pieces of literature in the field of IC, which includes different biological deployments are very limited [26]–[28]. In [26], [27], the authors have presented the IC of the DMC system under the binary coding scheme in absence of molecular noise. Further, Pierobon and Akyildiz in [28] have exploited the IC of the DMC system in closed form without any coding scheme but in presence of molecular noise.

As per the author's best knowledge, no reported literature includes cylindrical and spherical deployment for the analysis of SC in the DMC system. In [29], the authors have proposed the SC of the DMC system under rectangular deployment. Though, some partial results have been presented by the authors in [30], [31] to analyze IC and SC for the DMC system. However, these results are primary and are presented in the Conferences. Therefore, in this manuscript, we have extended the work reported in [29]–[31] by presenting various analytical expressions of IC and SC under the Biological Spherical Deployment (BSD) and Biological Cylindrical Deployment (BCD) of the DMC system. The author's contributions to this manuscript are summarized as follows

- For the first time, BSD and BCD schemes are used to present secrecy analysis of DMC system
- Presents analytical expressions of information capacity of DMC system under both BCD and BSD schemes.
- Presents analytical expressions of secrecy capacity of DMC system under both BCD and BSD schemes.
- Analyzes the effect of various parameters such as; Eve's distance, Eve's radius, the distance of authentic receiver, transmitted power, and BW, on secrecy capacity of the DMC system under BSD and BCD schemes.

Further, the manuscript is organized as follows. Section II presents a detailed description of the proposed system model. The mathematical expressions of the capacity for both the deployments are derived in Section III which is used to present secrecy capacity under BSD and BCD environments in Section IV. Section V presents numerical results. Finally, Section VI concludes the manuscript and recommends future directions.

II. SYSTEM MODEL

A DMC system employed for the evaluation of information-theoretical security, which provides the exact amount of the information received by 'Eve' during faithful communication link, under both the BSD and BCD schemes as shown in Fig. 1(a) and Fig. 1(b), respectively. In each of the cases, 'Alice' and 'Bob' are the transmitter bio-nano machine (T-BNM) and intended receiver BNM (R-BNM), respectively. Although the 'Eve' is an unintended or eavesdropping receiver, may be termed as 'Eves' BNM (E-BNM).

The amount of information received by 'Eve' is due to the leakage in the channel between 'Alice' and 'Bob', and hence termed as stolen information. 'Alice' is a point source located at an arbitrary point within the biological tissue irrespective of the deployment of either BCD or BSD. Alice releases information BNM (I-BNM) over the channel under a given deployment. During propagation, these I-BNMs are exposed to the degradation reaction, which is characterized by Brownian motion and mathematically given by Langevin equation [32]. Further, I-BNM binds with Bob upon reaching it and form receptor proteins. The amount of the information is proportional to the concentration of the incoming I-BNM. Finally, information is decoded by the Bob. Symbolically, X is defined as the number of particles emitted by Alice over the channel as a function of the time (denoted by n_t). Whereas, Y represents the number of particles, as a function of time, received at the Bob. And the number of particles received at Eve is denoted by Z. Also, the distance of Eve and Bob from the Alice are d_E and d_B, respectively. For notational distinctness in the derivation, d_B is taken as 'r' and 'd' in case of BSD and BCD schemes respectively.

Furthermore, in Fig. 1(a), a spherical tissue of radius R, azimuthally range ($0 \leq \varphi < 2\pi$) and elevation range ($0 \leq \theta < \pi$) is considered. Arbitrary coordinates of Alice, Bob, and Eve are A (r_{tx}, θ_{tx}, φ_{tx}), B (r_{rx}, θ_{rx} φ_{rx}) and E (r_{ex}, θ_{ex}, φ_{ex}) respectively. V_R is a spherical volume center at the receiver location with a radius $R_{VR} \ll d_E$. Whereas, in Fig. 1(b), a cylindrical tissue of radius ρ_c, azimuthally range, ($-\infty \leq z < +\infty$) and infinite height ($-\infty < z < +\infty$) is considered. Also, arbitrary coordinates of Alice, Bob and Eve are A (ρ_{tx}, φ_{tx}, z_{tx}), B (ρ_{rx}, φ_{rx}, z_{rx}) and E (ρ_{ex}, φ_{ex}, z_{ex}) respectively. Vρ is a spherical volume center at the receiver location with a radius $\rho_{V\rho} << d_E$, for clarity, we have used $\rho_{V\rho=R_{rx}}$ in the derivation. Finally, it is assumed that $v\hat{a}_z$ m/s is velocity of the flow. Where, $\hat{a}_z$ is a unit vector in the axial direction.

As mentioned, the CGF that is used to evaluate the IC and thereby SC depends on the biological structures of tissues.Therefore, in order to present the IC and in turn, SC under BSD and BCD as shown in Fig. 1(a) and Fig. 1(b), respectively [9], [11]. The CGF of diffusion for the system presented in Fig. 1(a), which follow asymmetry in all three dimensions and the reciprocity property (interchanging the location of transmitter and receiver does not change the information channel), can be given as [11],

$$c_{sph}\,(\mathrm{r},\mathrm{t}) = \sum_{\mathrm{K}=1}^{\infty} \mathrm{J}_0\,(\lambda_{\mathrm{k}}\mathrm{r})\,\mathrm{e}^{-\lambda_{\mathrm{k}}{}^2\mathrm{D}(\mathrm{t}-\mathrm{t}_0)}. \tag{1}$$

where, $c_{sph}(\mathrm{r},\mathrm{t})$ represents the concentration of molecules and $\mathrm{D}(m^2s^{-1})$ is the diffusion coefficient. Further, it is assumed that the I-BNMs are released from the T-BNM at time t_0 and received by R-BNM at time t. Symbol $J_n(.)$ represent the Bessel function of n^{th} order and first type for every positive value λ_n. Where, λ_n is the positive root of characteristic equation [11]. In case of BSD, λ_{nk} represents the k^{th} root of diffusion equation. However, for notational simplicity λ_{0k} is denoted as λ_k.

Now, taking Fourier Transform (FT) of Eq. (1)

$$C_{sph}\,(\mathrm{f}) = \int_0^{\infty} \mathrm{J}_0\,(\lambda_k \mathrm{r})\,\mathrm{e}^{-\lambda_{\mathrm{k}}{}^2\mathrm{D}(\mathrm{t}-\mathrm{t}_0)}\mathrm{e}^{-\mathrm{j}\omega}\mathrm{dt}. \tag{2}$$

where, $C_{sph}(\mathrm{f})$ represents FT of $c_{sph}(\mathrm{r},\mathrm{t})$.

Eq. (2) can be solved using [11] which gives:

$$C_{sph}(\mathrm{f}) = \frac{\mathrm{J}_0\,(\lambda_{\mathrm{k}}\mathrm{r})\,\mathrm{e}^{\lambda_{\mathrm{k}}{}^2\mathrm{D}(\mathrm{t}-\mathrm{t}_0)}}{\lambda_{\mathrm{k}}{}^2\mathrm{D}+\mathrm{j}\omega}. \tag{3}$$

In the preceding sections FT of Green's function, ($C_{sph}(\mathrm{f})$), is used to derive the expression of the IC and hence the SC under BSD. Further, the CGF of diffusion for the system presented in Fig. 1(b) follow asymmetry in all radial, azimuthal and axial coordinates for the $\rho_t x = 0$ and given as [9]:

$$c_{cyl}\,(r_{tx}, t_0) = \frac{1}{\sqrt{4\pi D\,(t-t_0)}} e^{\frac{-(\mathrm{d}-v(t-t_0))^2}{4D(t-t_0)} - k_d(t-t_0)} \times \sum_{\mathrm{m}=1}^{\infty} \frac{J_0\,(\lambda_{0m}\rho_{tx})\,J_0\,(\lambda_{0m}\rho)}{N_{0m}} \mathrm{e}^{-\gamma_{0m}{}^2(t-t_0)} u\,(\mathrm{t}-\mathrm{t}_0). \tag{4}$$

where, k_d (s^{-1}) is the reaction constant and ρ is the particle density. Also, for BCD defining the m^{th} root of diffusion equation as λ_{nm} and $\mathrm{N}_{nm} = \frac{\rho_c{}^2}{2} J_{\mathrm{n}}{}^2\,(\lambda_{nm}\rho_c) - J_{\mathrm{n}-1}\,(\lambda_{nm}\rho_c)\,J_{\mathrm{n}+1}\,(\lambda_{nm}\rho_c)$.

Further, the FT of $c_{cyl}(\mathrm{r},\mathrm{t})$ can be given as:

$$C_{cyl}\,(\mathrm{f}) = \frac{\mathrm{e}^{\left(-Dd^2-k_d-\mathrm{jd}v\right)(\mathrm{t}-\mathrm{t}_0)}}{2\pi} \frac{J_0\,(\lambda_{0m}\rho_{tx})\,J_0\,(\lambda_{0m}\rho)}{N_{0m}} \times \frac{e^{-\gamma_{0m}{}^2\mathrm{t}_0}}{\gamma_{0m}{}^2+j\omega}. \tag{5}$$

Again, in the preceding sections FT of Green's function, ($C_{cyl}(\mathrm{f})$), is used to derive expression of the information capacity and hence the secrecy capacity under BCD scheme.

III. CAPACITY UNDER DIFFERENT DEPLOYMENTS

In this section, the closed-form expressions of IC under BSD and BCD schemes have been derived.

A. CAPACITY UNDER BIOLOGICAL SPHERICAL DEPLOYMENT

In the case of BSD, the transmitted signal X is defined as the number of particles emitted into the space as a function of the time and is denoted by n_t. The received signal Y is a time-varying number of particles that are present inside a spherical volume V_R with center at the receiver location and with radius $\mathrm{R}_{VR} << \mathrm{r}$.

The capacity of the diffusion-based MC system in bits per second is calculated by maximizing the mutual information between the transmitted signal X and the received signal Y. Now, using the well-known expression of information capacity from Shannon [33].

$$\begin{aligned} \mathrm{C} &= \mathrm{I}(\mathrm{X};\mathrm{Y})_{\max} \\ &= \mathrm{I}\,(\mathrm{X};\rho) + \mathrm{I}\,(\mathrm{Y};\rho) - \mathrm{H}(\rho). \end{aligned} \tag{6}$$

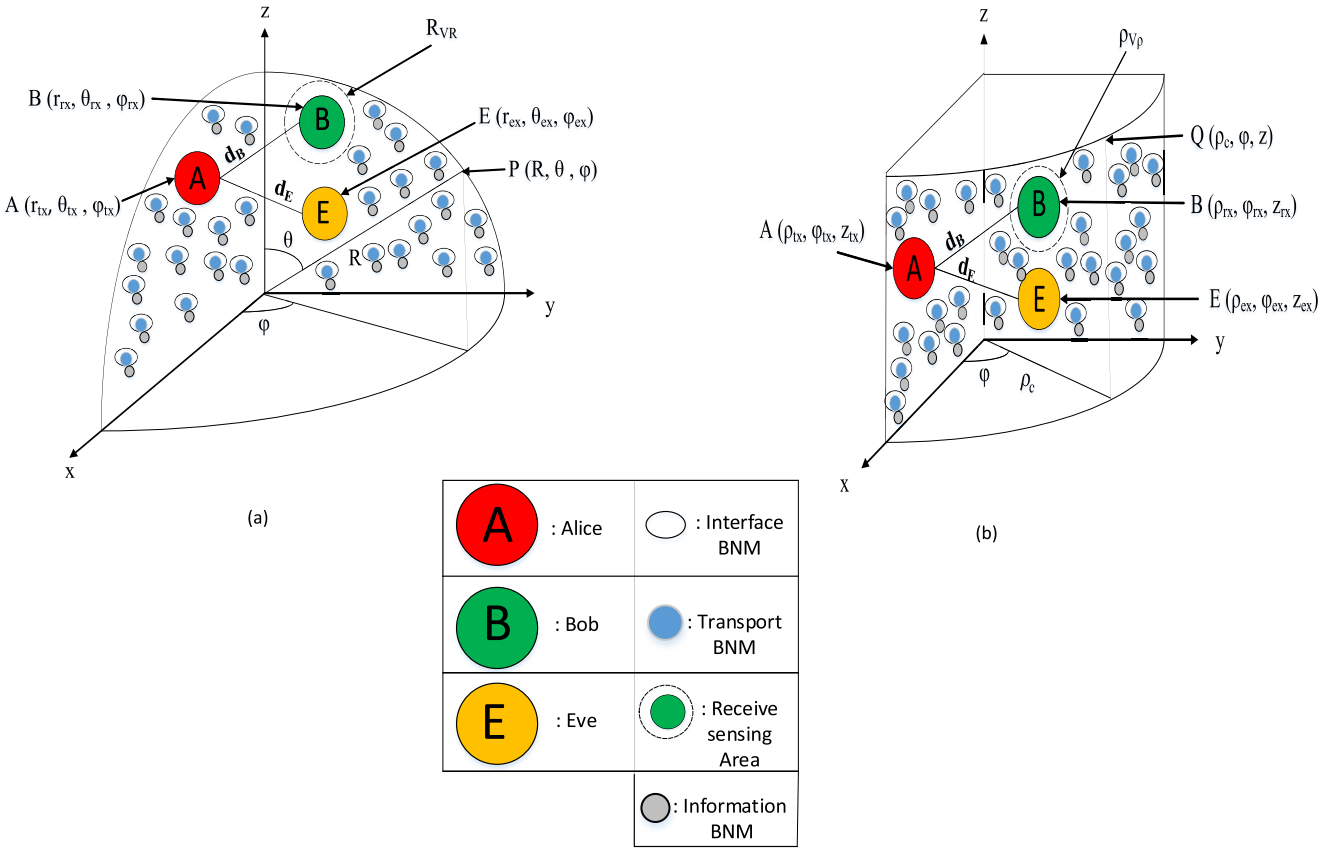

FIGURE 1. **Diffusive molecular communication under (a) BSD and (b) BCD.**

Now to obtain the mutual information I(X,Y) of the transmitted signal X and the received signal Y [28], we have to first find the mutual information I(X; ρ) (which includes Fick's diffusion) of the transmitted signal X given the particle distribution ρ.

$$I\,(\mathrm{X};\rho) = \mathrm{H}\,(\mathrm{X}) - \mathrm{H}\,(\mathrm{X}|\rho)\,. \tag{7}$$

where, H(X) = 2.W.H(η_t) is the entropy per second of the transmitted signal X. Whereas, $H\,(X \mid \rho)$ is the conditional entropy per second of the transmitted signal X given the particle distribution ρ.

After that, we have to find the mutual information $I\,(Y;\rho)$ of the received signal Y given the particle distribution ρ such that

$$I\,(Y;\rho) = \mathrm{H}\,(\rho) - \mathrm{H}\,(\rho|\mathrm{Y})\,. \tag{8}$$

where, $\mathrm{H}\,(\rho)$ is the conditional entropy per second of the particle distribution ρ given the received signal Y.

Now, in order to calculate $I\,(X;\rho)$ expression of $\mathrm{H}\,(X|\rho)$ is required. Stepwise derivation for $\mathrm{H}\,(X|\rho)$ is given in Appendix A. Now, substituting the value of $\mathrm{H}\,(X|\rho)$ in Eq. (7) and after some mathematical steps we get $\mathrm{I}\,(X;\rho)$ as:

$$\begin{aligned}\mathrm{I}\,(\mathrm{X};\rho) = {} & 2\mathrm{WH}\,(\eta_t) - \frac{1}{\mathrm{w}}\log\left(\lambda_k{}^2\mathrm{D}\right)^2 - \sum_{i=1}^{\infty}\left(\frac{2\pi}{\lambda_k{}^2.\mathrm{D}}\right)^{2i} \\ & \times \frac{(-1)^{i+1}}{(2i+1)\,i}.\left(\frac{\mathrm{W}}{2\pi}\right)^{2i+1} \\ & + \log\,(2) + 2\log_2\left(\mathrm{J}_0\,(\lambda_k r)\,.e^{\lambda_k{}^2.\mathrm{D}.t_0}\right).\end{aligned} \tag{9}$$

Further, using the CGF of spherical environment from Eq. (3) and following [33], the entropy per second of the particle distribution $H\,(\rho)$ is given as:

$$\begin{aligned}\mathrm{H}\,(\rho) &= \mathrm{H}\,(\mathrm{X}) + \mathrm{H}\,(\rho|\mathrm{X}) - \mathrm{H}\,(X \mid \rho) \\ &= 2\mathrm{W.H}\,(\eta_t) - \frac{1}{\mathrm{W}}\log\left(\lambda_k{}^2\mathrm{D}\right)^2 \\ &\quad - \sum_{i=1}^{\infty}\left(\frac{2\pi}{\lambda_k{}^2.\mathrm{D}}\right)^{2i}\frac{(-1)^{i+1}}{(2i+1)\,.i}.\left(\frac{\mathrm{W}}{2\pi}\right)^{2i+1} \\ &\quad + \log\,(2) + 2\log_2\left(J_0\,(\lambda_k r)\,e^{\lambda_k{}^2.\mathrm{D}t_0}\right).\end{aligned} \tag{10}$$

In Eq. (10), $\mathrm{H}\,(\rho|\mathrm{X})$ is the conditional entropy per second of the particle distribution given the transmitted signal X. For given transmitted signal X, as the input of the Fick's diffusion, the output particle distribution ρ is completely known and hence $\mathrm{H}\,(\rho|\mathrm{X}) = 0$.

Further, in order to calculate $\mathrm{I}(Y;\rho)$ expression of $\mathrm{H}(\rho|\mathrm{X})$ is required. Stepwise derivation for $\mathrm{H}(\rho|\mathrm{X})$ is given in Appendix B. Now, substituting the value of $\mathrm{H}(\rho|\mathrm{X})$ and Eq. (10) into Eq. (8) we get $\mathrm{I}(Y;\rho)$ as:

$$\begin{aligned}\mathrm{I}(Y;\rho) &= 2\mathrm{W}.\mathrm{H}(\eta_t) - \frac{1}{\mathrm{W}}\log\left(\lambda_k{}^2\mathrm{D}\right)^2 - \sum_{i=1}^{\infty}\left(\frac{2\pi}{\lambda_k{}^2.\mathrm{D}}\right)^{2i} \\ &\times \frac{(-1)^{i+1}}{(2i+1).i}.\left(\frac{\mathrm{W}}{2\pi}\right)^{2i+1} + \log(2) \\ &+ 2\log_2\left(J_0(\lambda_k r)\, e^{\lambda_k{}^2.\mathrm{D}t_0}\right) \\ &- 2W\frac{2\pi}{3}\frac{\mathrm{E}[n_t]\,\mathrm{R_{VR}}J_0(\lambda_k r)e^{\lambda_k{}^2\mathrm{D}(t-t_0)}}{\mathrm{W}\lambda_k{}^2} \\ &- 2W\ln(2\mathrm{W}\tau_p) \\ &- 2W ln\left(\Gamma\left(\frac{2\pi}{3}\frac{\mathrm{E}[n_t]\,\mathrm{R_{VR}}J_0(\lambda_k r)e^{\lambda_k{}^2\mathrm{D}(t-t_0)}}{\mathrm{W}\lambda_k{}^2}\right)\right) \\ &- 2W\left(1 - \frac{2\pi}{3}\frac{\mathrm{E}[n_t]\,\mathrm{R_{VR}}J_0(\lambda_k r)e^{\lambda_k{}^2\mathrm{D}(t-t_0)}}{\mathrm{W}\lambda_k{}^2}\right) \\ &\times \psi\left(\frac{2\pi}{3}\frac{\mathrm{E}[n_t]\,\mathrm{R_{VR}}J_0(\lambda_k r)e^{\lambda_k{}^2\mathrm{D}(t-t_0)}}{\mathrm{W}\lambda_k{}^2}\right). \quad (11)\end{aligned}$$

Here, $\mathrm{R_{VR}}$ is the radius of spherical receiver with volume V_R, ρ is the particle distribution, W is the bandwidth and $\psi(.)$ is the Digamma function. Substituting Eq. (9), Eq. (10), and Eq. (11) into Eq. (6) we get:

$$\begin{aligned}\mathrm{C_{sph}} &= 2\mathrm{W}.\mathrm{H}(\eta_t) - \frac{1}{\mathrm{W}}\log\left(\lambda_k{}^2\mathrm{D}\right)^2 - \sum_{i=1}^{\infty}\left(\frac{2\pi}{\lambda_k{}^2.\mathrm{D}}\right)^{2i} \\ &\times \frac{(-1)^{i+1}}{(2i+1).i}.\left(\frac{\mathrm{W}}{2\pi}\right)^{2i+1} + \log(2) \\ &+ 2\log_2\left(J_0(\lambda_k r)\, e^{\lambda_k{}^2.\mathrm{D}t_0}\right) \\ &- 2W\frac{2\pi}{3}\frac{\mathrm{E}[n_t]\,\mathrm{R_{VR}}J_0(\lambda_k r)e^{\lambda_k{}^2\mathrm{D}(t-t_0)}}{\mathrm{W}\lambda_k{}^2} \\ &- 2W\ln(2\mathrm{W}\tau_p) \\ &- 2W ln\left(\Gamma\left(\frac{2\pi}{3}\frac{\mathrm{E}[n_t]\,\mathrm{R_{VR}}J_0(\lambda_k r)e^{\lambda_k{}^2\mathrm{D}(t-t_0)}}{\mathrm{W}\lambda_k{}^2}\right)\right) \\ &- 2W\left(1 - \frac{2\pi}{3}\frac{\mathrm{E}[n_t]\,\mathrm{R_{VR}}J_0(\lambda_k r)e^{\lambda_k{}^2\mathrm{D}(t-t_0)}}{\mathrm{W}\lambda_k{}^2}\right) \\ &\times \psi\left(\frac{2\pi}{3}\frac{\mathrm{E}[n_t]\,\mathrm{R_{VR}}J_0(\lambda_k r)e^{\lambda_k{}^2\mathrm{D}(t-t_0)}}{\mathrm{W}\lambda_k{}^2}\right). \quad (12)\end{aligned}$$

Further, we have average number of emitted particles, $\mathrm{E}(\eta_t) = (\mathrm{P}_H)/3.\mathrm{W}.\mathrm{K}_b.\mathrm{T}$ with P_H as the average thermodynamic power spent. Also, entropy of the number of emitted particles per time sample is, $\mathrm{H}(\mathrm{n}_t) = 1 + \log_2 \mathrm{E}[\mathrm{n}_t]$ [11]. Substituting these values in Eq. (12) the final expression of the capacity of DMC under BSD can be given as:

$$\begin{aligned}C_{sph} &= 2W.\left(1 + \log_2\frac{\mathrm{P_H}}{3\mathrm{WK_bT}}\right) - \frac{1}{\mathrm{W}}\log\left(\lambda_k{}^2\mathrm{D}\right)^2 \\ &- \sum_{i=1}^{\infty}\left(\frac{2\pi}{\lambda_k{}^2.\mathrm{D}}\right)^{2i} \times \frac{(-1)^{i+1}}{(2i+1).i}.\left(\frac{\mathrm{W}}{2\pi}\right)^{2i+1} + \log(2) \\ &+ 2\log_2\left(J_0(\lambda_k r)\, e^{\lambda_k{}^2.\mathrm{D}t_0}\right) \\ &- 2\mathrm{W}\frac{2\pi}{9}\frac{\mathrm{P_H}}{W^2\mathrm{K_bT}}\frac{\mathrm{R_{VR}}J_0(\lambda_k r)e^{\lambda_k{}^2\mathrm{D}(t-t_0)}}{\mathrm{W}\lambda_k{}^2} \\ &- 2W\ln(2\mathrm{W}\tau_p) \\ &- 2W ln\left(\Gamma\left(\frac{2\pi}{9}\frac{\mathrm{P_H}}{W^2\mathrm{K_bT}}\frac{\mathrm{R_{VR}}J_0(\lambda_k r)e^{\lambda_k{}^2\mathrm{D}(t-t_0)}}{\mathrm{W}\lambda_k{}^2}\right)\right) \\ &- 2W\left(1 - \frac{2\pi}{9}\frac{\mathrm{P_H}}{W^2\mathrm{K_bT}}\frac{\mathrm{R_{VR}}J_0(\lambda_k r)e^{\lambda_k{}^2\mathrm{D}(t-t_0)}}{\mathrm{W}\lambda_k{}^2}\right) \\ &\times \psi\left(\frac{2\pi}{9}\frac{\mathrm{P_H}}{W^2\mathrm{K_bT}}\frac{\mathrm{R_{VR}}\,J_0(\lambda_k r)e^{\lambda_k{}^2\mathrm{D}(t-t_0)}}{\mathrm{W}\lambda_k{}^2}\right). \quad (13)\end{aligned}$$

B. CAPACITY UNDER BIOLOGICAL CYLINDRICAL DEPLOYMENT

Capacity under biological cylindrical deployment can be evaluated using very similar steps as used in case of biological spherical deployment.

Once again, in case of biological cylindrical deployment, in order to calculate $I(X;\rho)$, expression of $H(X|\rho)$ is required. However, derivation for $H(X|\rho)$ is given in Appendix C. Further, substituting the value of $H(X|\rho)$ in Eq. (7) and after some mathematical steps we get $H(X;\rho)$ as:

$$\begin{aligned}I(\mathrm{X};\rho) &= 2\mathrm{WH}(\eta_t) - \frac{1}{\mathrm{W}}\log\left(\gamma_{0\mathrm{m}}{}^2\right)^2 - \sum_{i=1}^{\infty}\left(\frac{2\pi}{\lambda_k{}^2.\mathrm{D}}\right)^{2i} \\ &\times \frac{(-1)^{i+1}}{(2i+1)\,i}.\left(\frac{\mathrm{W}}{2\pi}\right)^{2i+1} + \log(2) + 2\log_2 \\ &\times \left(\frac{J_0(\lambda_{0m}\rho_{tx})\,J_0(\lambda_{0m}\rho)}{2\pi N_{0m}} e^{-(D\mathrm{d}^2+k_d+\gamma_{0m}{}^2)t_0}\right). \quad (14)\end{aligned}$$

Further, in order to calculate $I(Y;\rho)$ expression of $H(\rho|Y)$ is required which has been derived in Appendix D. Also, expression for $\mathrm{H}(\rho)$ has been presented in Appendix C. Now, substituting $\mathrm{H}(\rho)$ and $H(\rho|Y)$ from Appendix C and Appendix D respectively into Eq. (8) we get $I(Y;\rho)$ as:

$$\begin{aligned}I(Y;\rho) &= 2\mathrm{W}.\mathrm{H}(\eta_t) - \frac{1}{\mathrm{W}}\log\left(\gamma_{0\mathrm{m}}{}^2\right)^2 \\ &- \sum_{i=1}^{\infty}\left(\frac{2\pi}{\lambda_k{}^2.\mathrm{D}}\right)^{2i}.\frac{(-1)^{i+1}}{(2i+1)\,i}.\left(\frac{\mathrm{W}}{2\pi}\right)^{2i+1} \\ &+ \log(2) + 2\log_2 \\ &\times \left(\frac{J_0(\lambda_{0m}\rho_{tx})\,J_0(\lambda_{0m}\rho)}{2\pi N_{0m}} e^{-(D\mathrm{d}^2+k_d+\gamma_{0m}{}^2)t_0}\right) \\ &- 2W\frac{DR_{rx}E[n_t]}{3W\gamma_{0m}{}^2}\frac{J_0(\lambda_{0m}\rho_{tx})\,J_0(\lambda_{0m}\rho)}{N_{0m}}\end{aligned}$$

$$\times e^{\left(-D\mathrm{d}^2-k_d-j\mathrm{d}v-{\gamma_{0m}}^2\right)(\mathrm{t}-\mathrm{t}_0)} - 2\mathrm{W}\ln\left(2\mathrm{W}\tau_\mathrm{p}\right) - 2W\ ln\left(\Gamma\left(\frac{DR_{rx}E\left[n_t\right]}{3W{\gamma_{0m}}^2}\frac{J_0\left(\lambda_{0m}\rho_{tx}\right)J_0\left(\lambda_{0m}\rho\right)}{N_{0m}} \times e^{\left(-D\mathrm{d}^2-k_d-j\mathrm{d}v-{\gamma_{0m}}^2\right)(\mathrm{t}-\mathrm{t}_0)}\right)\right) - 2W\left(1-\frac{DR_{rx}E\left[n_t\right]}{3W{\gamma_{0m}}^2}\frac{J_0\left(\lambda_{0m}\rho_{tx}\right)J_0\left(\lambda_{0m}\rho\right)}{N_{0m}} \times e^{\left(-D\mathrm{d}^2-k_d-j\mathrm{d}v-{\gamma_{0m}}^2\right)(\mathrm{t}-\mathrm{t}_0)}\right) \times \psi\left(\frac{DR_{rx}E\left[n_t\right]}{3W{\gamma_{0m}}^2}\frac{J_0\left(\lambda_{0m}\rho_{tx}\right)J_0\left(\lambda_{0m}\rho\right)}{N_{0m}} \times e^{\left(-D\mathrm{d}^2-k_d-j\mathrm{d}v-{\gamma_{0m}}^2\right)(\mathrm{t}-\mathrm{t}_0)}\right). \quad (15)$$

Here, R_{rx} is the radius of cylindrical receiver. Now, substituting Eq. (14), Eq. (15) and value of $H(\rho)$ (Refer Appendix C) into Eq. (6) we get the expression of capacity as:

$$C_{cyl} = 2\mathrm{W.H}\left(\eta_\mathrm{t}\right) - \frac{1}{\mathrm{W}}\log\left({\gamma_{0\mathrm{m}}}^2\right)^2 - \sum_{\mathrm{i}=1}^{\infty}\left(\frac{2\pi}{{\lambda_\mathrm{k}}^2.\mathrm{D}}\right)^{2\mathrm{i}}.\frac{(-1)^{\mathrm{i}+1}}{(2\mathrm{i}+1)\,\mathrm{i}}.\left(\frac{\mathrm{W}}{2\pi}\right)^{2\mathrm{i}+1} + \log(2) + 2\log_2 \times \left(\frac{J_0\left(\lambda_{0m}\rho_{tx}\right)J_0\left(\lambda_{0m}\rho\right)}{2\pi N_{0m}}e^{-\left(Dd^2+k_d+{\gamma_{0m}}^2\right)t_0}\right) - 2W\frac{DR_{rx}E\left[n_t\right]}{3W{\gamma_{0m}}^2}\frac{J_0\left(\lambda_{0m}\rho_{tx}\right)J_0\left(\lambda_{0m}\rho\right)}{N_{0m}} \times e^{\left(-D\mathrm{d}^2-k_d-j\mathrm{d}v-{\gamma_{0m}}^2\right)(\mathrm{t}-\mathrm{t}_0)} - 2\mathrm{W}\ln\left(2\mathrm{W}\tau_\mathrm{p}\right) - 2W\ ln \times \left(\Gamma\left(\frac{DR_{rx}E\left[n_t\right]}{3W{\gamma_{0m}}^2}\frac{J_0\left(\lambda_{0m}\rho_{tx}\right)J_0\left(\lambda_{0m}\rho\right)}{N_{0m}} \times e^{\left(-D\mathrm{d}^2-k_d-j\mathrm{d}v-{\gamma_{0m}}^2\right)(\mathrm{t}-\mathrm{t}_0)}\right)\right) - 2W\left(1-\frac{DR_{rx}E\left[n_t\right]}{3W{\gamma_{0m}}^2}\frac{J_0\left(\lambda_{0m}\rho_{tx}\right)J_0\left(\lambda_{0m}\rho\right)}{N_{0m}} \times e^{\left(-D\mathrm{d}^2-k_d-j\mathrm{d}v-{\gamma_{0m}}^2\right)(\mathrm{t}-\mathrm{t}_0)}\right) \times \psi\left(\frac{DR_{rx}E\left[n_t\right]}{3W{\gamma_{0m}}^2}\frac{J_0\left(\lambda_{0m}\rho_{tx}\right)J_0\left(\lambda_{0m}\rho\right)}{N_{0m}} \times e^{\left(-D\mathrm{d}^2-k_d-j\mathrm{d}v-{\gamma_{0m}}^2\right)(\mathrm{t}-\mathrm{t}_0)}\right). \quad (16)$$

With the suitable substitution, we get the final expression of the capacity of DMC under the BCD as:

$$C_{cyl} = 2W.\left(1+\log_2\frac{\mathrm{P_H}}{3\mathrm{WK_bT}}\right) - \frac{1}{\mathrm{W}}\log\left({\gamma_{0\mathrm{m}}}^2\right)^2 - \sum_{\mathrm{i}=1}^{\infty}\left(\frac{2\pi}{{\lambda_\mathrm{k}}^2.\mathrm{D}}\right)^{2\mathrm{i}}.\frac{(-1)^{\mathrm{i}+1}}{(2\mathrm{i}+1)\,\mathrm{i}}.\left(\frac{\mathrm{W}}{2\pi}\right)^{2\mathrm{i}+1} + \log(2) + 2\log_2 \times \left(\frac{J_0\left(\lambda_{0m}\rho_{tx}\right)J_0\left(\lambda_{0m}\rho\right)}{2\pi N_{0m}}e^{-\left(D\mathrm{d}^2+k_d+{\gamma_{0m}}^2\right)t_0}\right) - 2W\frac{DR_{rx}}{3W{\gamma_{0m}}^2}\frac{\mathrm{P_H}}{3\mathrm{WK_bT}}\frac{J_0\left(\lambda_{0m}\rho_{tx}\right)J_0\left(\lambda_{0m}\rho\right)}{N_{0m}} \times e^{\left(-D\mathrm{d}^2-k_d-j\mathrm{d}v-{\gamma_{0m}}^2\right)(\mathrm{t}-\mathrm{t}_0)} - 2\mathrm{W}\ln\left(2\mathrm{W}\tau_\mathrm{p}\right) - 2W\ ln \times \left(\Gamma\left(\frac{DR_{rx}}{3W{\gamma_{0m}}^2}\frac{\mathrm{P_H}}{3\mathrm{WK_bT}}\frac{J_0\left(\lambda_{0m}\rho_{tx}\right)J_0\left(\lambda_{0m}\rho\right)}{N_{0m}} \times e^{\left(-D\mathrm{d}^2-k_d-j\mathrm{d}v-{\gamma_{0m}}^2\right)(\mathrm{t}-\mathrm{t}_0)}\right)\right) - 2W\left(1-\frac{DR_{rx}}{3W{\gamma_{0m}}^2}\frac{\mathrm{P_H}}{3\mathrm{WK_bT}}\frac{J_0\left(\lambda_{0m}\rho_{tx}\right)J_0\left(\lambda_{0m}\rho\right)}{N_{0m}} \times e^{\left(-D\mathrm{d}^2-k_d-j\mathrm{d}v-{\gamma_{0m}}^2\right)(\mathrm{t}-\mathrm{t}_0)}\right) \times \psi\left(\frac{DR_{rx}}{3W{\gamma_{0m}}^2}\frac{\mathrm{P_H}}{3\mathrm{WK_bT}}\frac{J_0\left(\lambda_{0m}\rho_{tx}\right)J_0\left(\lambda_{0m}\rho\right)}{N_{0m}} \times e^{\left(-D\mathrm{d}^2-k_d-j\mathrm{d}v-{\gamma_{0m}}^2\right)(\mathrm{t}-\mathrm{t}_0)}\right). \quad (17)$$

IV. SECRECY CAPACITY UNDER DIFFERENT DEPLOYMENTS

In this section analytical expressions of SC under BSD and BCD schemes have been derived. The secrecy capacity of the diffusion-based channel is derived as the maximum of the difference between the mutual information of the authentic communication link and the information leakage (the amount of information "stolen" by Eve). Thus, the secrecy capacity [29] is

$$C_s = max\left[(X;Y) - I(X;Z)\right] = C_B - C_E. \quad (18)$$

where, C_B and C_E are the capacity of authentic channel (Bob) and Eve's channel respectively and Z is the signal observed by Eve (eavesdropper). From [29], SC cannot be less than 0, C_s can be given as:

$$C_s = max\left[0,(X;Y) - I(X;Z)\right] = C_B - C_E. \quad (19)$$

A. SECRECY CAPACITY UNDER BIOLOGICAL SPHERICAL ENVIRONMENT

Furthermore, Eq. (13) can also be rewritten as:

$$C_{sph} = 2\mathrm{W.H}\left(\eta_\mathrm{t}\right) - \frac{1}{\mathrm{W}}\log\left({\lambda_\mathrm{k}}^2\mathrm{D}\right)^2 - \sum_{\mathrm{i}=1}^{\infty}\left(\frac{2\pi}{{\lambda_\mathrm{k}}^2.\mathrm{D}}\right)^{2\mathrm{i}}\frac{(-1)^{\mathrm{i}+1}}{(2\mathrm{i}+1)\,.\mathrm{i}} \times .\left(\frac{\mathrm{W}}{2\pi}\right)^{2\mathrm{i}+1} + \log 2 + 2\log_2\left(J_0\left(\lambda_\mathrm{k}\mathrm{r}\right)e^{{\lambda_\mathrm{k}}^2.\mathrm{Dt}_0}\right) - 2W\eta - 2W\ln\left(2\mathrm{W}\tau_\mathrm{p}\right) - 2W\ln\left(\Gamma\left(\eta\right)\right) - 2W\left(1-\eta\right)\psi\left(\eta\right). \quad (20)$$

where, $\eta = \frac{2\pi}{3}\frac{\mathrm{E}[n_t]\mathrm{R_{VR}}\mathrm{J}_0(\lambda_\mathrm{k}r)e^{{\lambda_\mathrm{k}}^2\mathrm{D}(\mathrm{t}-\mathrm{t}_0)}}{W{\lambda_\mathrm{k}}^2}$ and $\tau_\mathrm{p} = \frac{{\mathrm{R_{VR}}}^2}{D}$, is the time interval in which we consider a quasi-constant particle distribution.

This leads to:

$$C_{sph} = 2\mathrm{W}\left(1+\log_2\frac{\mathrm{P_H}}{3\mathrm{WK_bT}}\right) - \frac{1}{\mathrm{W}}\log\left({\lambda_\mathrm{k}}^2\mathrm{D}\right)^2 - \sum_{\mathrm{i}=1}^{\infty}\left(\frac{2\pi}{{\lambda_\mathrm{k}}^2.\mathrm{D}}\right)^{2\mathrm{i}}\frac{(-1)^{\mathrm{i}+1}}{(2\mathrm{i}+1)\,.\mathrm{i}}.\left(\frac{\mathrm{W}}{2\pi}\right)^{2\mathrm{i}+1} + \log 2 + 2\log_2\left(J_0\left(\lambda_\mathrm{k}\mathrm{r}\right)\mathrm{e}^{{\lambda_\mathrm{k}}^2.\mathrm{Dt_0}}\right) - 2W\eta - 2W\ln\left(2\mathrm{W}\frac{{\mathrm{R_{VR}}}^2}{D}\right) - 2W\ln\left(\Gamma\left(\eta\right)\right) - 2W\left(1-\eta\right)\psi\left(\eta\right). \quad (21)$$

Both C_B and C_E can be calculated by using Eq. (21). Now, the capacity of the authentic receiver is:

$$C_\mathrm{B} = 2\mathrm{W}\left(1+\log_2\frac{\mathrm{P_H}}{3\mathrm{WK_bT}}\right) - \frac{1}{\mathrm{W}}\log\left({\lambda_\mathrm{k}}^2\mathrm{D}\right)^2 - \sum_{\mathrm{i}=1}^{\infty}\left(\frac{2\pi}{{\lambda_\mathrm{k}}^2.\mathrm{D}}\right)^{2\mathrm{i}}\frac{(-1)^{\mathrm{i}+1}}{(2\mathrm{i}+1)\,.\mathrm{i}}.\left(\frac{\mathrm{W}}{2\pi}\right)^{2\mathrm{i}+1} + \log 2 + 2\log_2\left(J_0\left(\lambda_\mathrm{k}r_B\right)\mathrm{e}^{{\lambda_\mathrm{k}}^2.\mathrm{Dt_0}}\right) - 2W\eta_B - 2W\ln\left(2\mathrm{W}\frac{{\mathrm{R_{VRB}}}^2}{D}\right) - 2W\ln\left(\Gamma\left(\eta_B\right)\right) - 2W\left(1-\eta_B\right)\psi\left(\eta_B\right). \quad (22)$$

where, $\eta_B = \frac{2\pi}{9}\frac{P_H}{W^2K_bT}\frac{\mathrm{R_{VRB}J_0(\lambda_k r_B)e^{\lambda_k{}^2D(t-t_0)}}}{{\lambda_\mathrm{k}}^2}$.

Similarly, C_E can also be obtained. Finally, the secrecy capacity of the system is:

$$C_s|sph = 2\log_2\left(\frac{J_0(\lambda_\mathrm{k}r_B)}{J_0(\lambda_\mathrm{k}r_E)}\right) + 2W\left(\eta_E-\eta_B\right) + 2W\ln\left(\frac{{\mathrm{R_{VRE}}}^2}{{\mathrm{R_{VRB}}}^2}\right) + 2W\ln\left(\frac{\Gamma\left(\eta_E\right)}{\Gamma\left(\eta_B\right)}\right) + 2W\left[(1-\eta_E)\,\psi\left(\eta_E\right)-(1-\eta_B)\,\psi\left(\eta_B\right)\right]. \quad (23)$$

It is noteworthy to mention that Eq. (23) represent the secrecy capacity of DMC system under biological spherical environment. Also, Eq. (23) can be treated as modification over secrecy expression presented by Lorenzo Muchhi *et. al.* in [29].

B. SECRECY CAPACITY UNDER BIOLOGICAL CYLINDRICAL ENVIRONMENT

Moreover, Eq. (17) can also be rewritten as:

$$C_{cyl} = 2\mathrm{W.H}\left(\eta_\mathrm{t}\right) - \frac{1}{\mathrm{W}}\log\left({\gamma_\mathrm{0m}}^2\right)^2 - \sum_{\mathrm{i}=1}^{\infty}\left(\frac{2\pi}{{\lambda_\mathrm{k}}^2.\mathrm{D}}\right)^{2\mathrm{i}}\frac{(-1)^{\mathrm{i}+1}}{(2\mathrm{i}+1)\,.\mathrm{i}}.\left(\frac{\mathrm{W}}{2\pi}\right)^{2\mathrm{i}+1} + \log 2 + 2\log_2\left(\frac{J_0\left(\lambda_{0m}\rho_{tx}\right)J_0\left(\lambda_{0m}\rho\right)}{2\pi N_{0m}}\mathrm{e}^{-\left(D\mathrm{d}^2+k_d+{\gamma_{0m}}^2\right)t_0}\right) - 2W\eta - 2W\ln\left(2\mathrm{W}\tau_\mathrm{p}\right) - 2W\ln\left(\Gamma\left(\eta\right)\right) - 2W\left(1-\eta\right)\psi\left(\eta\right). \quad (24)$$

TABLE 1. Parameters used in analytical results.

Parameter	Variable	Value
System temperature	T	298.15°K
Diffusion coefficient	D	$10^{-9}\mathrm{m^2s^{-1}}$
Boltzmann constant	K_b	$1.380650424\times10^{-23}$ J/K
Radius of the spherical receiver volume	R_{VR}	10 nm
Average thermodynamic power	P_H	1-4 pW
Bandwidth	W	10-60 Hz
Roots of Diffusion Equation	λ_{nk} or λ_{nm}	0.1×10^{-12} - 1×10^{-12} m
Time	$t-t_0$	10μs
Cylinder radius	ρ_c	5,10,15 μm
Point source Tx location for cylindrical	$(\rho_{tx}, z_{tx}, \phi_{tx})$	(3μm,0,0)
Degradation reaction constant in cylinder	k_d	0, 20 $\mathrm{s^{-1}}$
Radius of the Cylindrical receiver volume	R_{rx}	1.5 μm

where, $\eta = \frac{DR_{rx}E[n_t]}{3W{\gamma_{0m}}^2}\frac{J_0(\lambda_{0m}\rho_{tx})J_0(\lambda_{0m}\rho)}{N_{0m}} \times \mathrm{e}^{\left(-D\mathrm{d}^2-k_d-j\mathrm{d}v-{\gamma_{0m}}^2\right)(\mathrm{t}-\mathrm{t_0})}$

These yields,

$$C_{cyl} = 2\mathrm{W}\left(1+\log_2\frac{\mathrm{P_H}}{3\mathrm{WK_bT}}\right) - \frac{1}{\mathrm{W}}\log\left({\gamma_\mathrm{0m}}^2\right)^2 - \sum_{\mathrm{i}=1}^{\infty}\left(\frac{2\pi}{{\lambda_\mathrm{k}}^2.\mathrm{D}}\right)^{2\mathrm{i}}\times\frac{(-1)^{\mathrm{i}+1}}{(2\mathrm{i}+1)\,.\mathrm{i}}.\left(\frac{\mathrm{W}}{2\pi}\right)^{2\mathrm{i}+1} + \log 2 + 2\log_2\left(\frac{J_0\left(\lambda_{0m}\rho_{tx}\right)J_0\left(\lambda_{0m}\rho\right)}{2\pi N_{0m}}\mathrm{e}^{-\left(D\mathrm{d}^2+k_d+{\gamma_{0m}}^2\right)t_0}\right) - 2W\eta - 2W\ln\left(2\mathrm{W}\frac{{\mathrm{R_{rx}}}^2}{D}\right) - 2W\ln\left(\Gamma\left(\eta\right)\right) - 2W\left(1-\eta\right)\psi\left(\eta\right). \quad (25)$$

Now, the capacity of authentic receiver is:

$$C_{\boldsymbol{B}} = 2\mathrm{W}\left(1+\log_2\frac{\mathrm{P_H}}{3\mathrm{WK_bT}}\right) - \frac{1}{\mathrm{W}}\log\left({\gamma_\mathrm{0m}}^2\right)^2 - \sum_{\mathrm{i}=1}^{\infty}\left(\frac{2\pi}{{\lambda_\mathrm{k}}^2.\mathrm{D}}\right)^{2\mathrm{i}}\frac{(-1)^{\mathrm{i}+1}}{(2\mathrm{i}+1)\,.\mathrm{i}}.\left(\frac{\mathrm{W}}{2\pi}\right)^{2\mathrm{i}+1} + \log 2 + 2\log_2\left(\frac{J_0\left(\lambda_{0m}\rho_{tx}\right)J_0\left(\lambda_{0m}\rho\right)}{2\pi N_{0m}}\mathrm{e}^{-\left(D{d_B}^2+k_d+{\gamma_{0m}}^2\right)t_0}\right) - 2W\eta_B - 2W\ln\left(2\mathrm{W}\frac{{\mathrm{R_{rx}}}^2}{D}\right) - 2W\ln\left(\Gamma\left(\eta_B\right)\right) - 2W\left(1-\eta_B\right)\psi\left(\eta_B\right). \quad (26)$$

where, $\eta_B = \frac{DR_{rxB}}{9\,{\gamma_{0m}}^2}\frac{\mathrm{P_H}}{\mathrm{W^2K_bT}}\frac{J_0(\lambda_{0m}\rho_{tx})J_0(\lambda_{0m}\rho)}{N_{0m}} \times \mathrm{e}^{-\left(D{d_B}^2+k_d+{\gamma_{0m}}^2\right)t_0}$

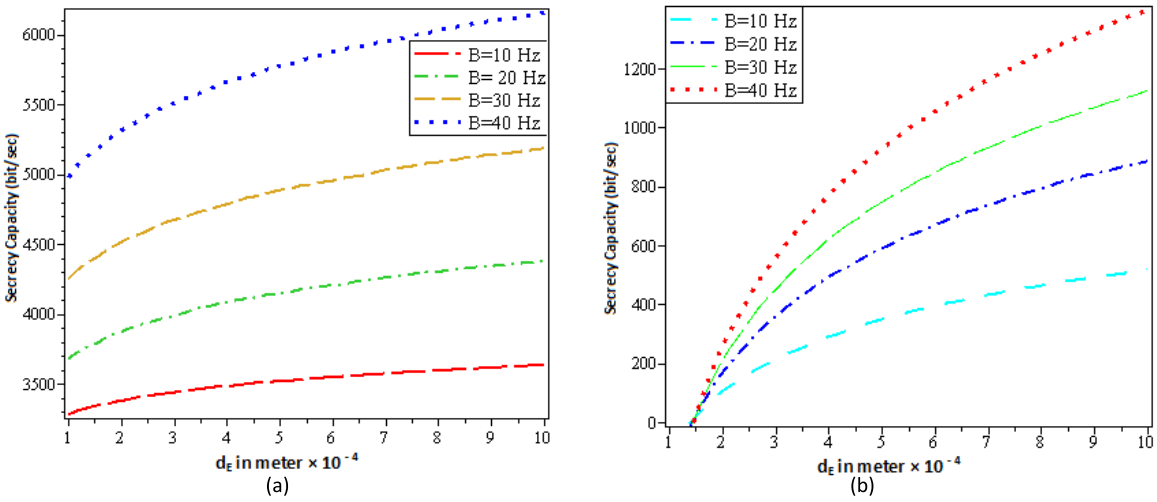

FIGURE 2. The response of Eve's distance over secrecy capacity for different values of BW and transmit power equal to 10^{-12} W under (a) BCD and (b) BSD.

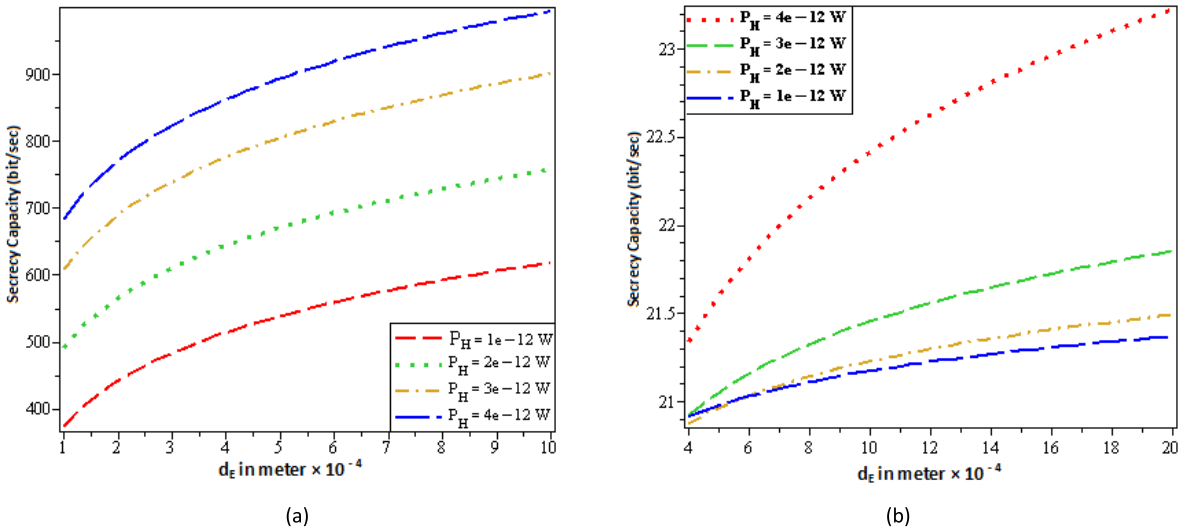

FIGURE 3. The response of Eve's distance over secrecy capacity for different values of transmit power and BW equal to 10 Hz under (a) BCD and (b) BSD.

Similarly, C_E can also be obtained. Finally, the secrecy capacity of the BCD is:

$$C_s|cyl = 2\log_2\left(e^{(d_E{}^2-d_B{}^2)Dt_0}\right) + 2W(\eta_E - \eta_B) + 2W\ln\left(\frac{R_{rxE}{}^2}{R_{rxB}{}^2}\right) + 2W\ln\left(\frac{\Gamma(\eta_E)}{\Gamma(\eta_B)}\right) + 2W\left[(1-\eta_E)\psi(\eta_E) - (1-\eta_B)\psi(\eta_B)\right]. \quad (27)$$

It is noteworthy to mention that Eq. (27) represent the secrecy capacity of DMC system under biological cylindrical environment. Also, Eq. (27) is novel and never represented in the available literatures.

V. NUMERICAL RESULTS

In this section, the proposed secrecy capacity under different biological structures, namely biological cylindrical and biological spherical structures have been presented numerically. SC has been analyzed against Eve's distance and Eve's radius for different values of the power and/or bandwidth. Different parameters used in the analysis along with respective values have been listed in Table 1.

Fig. 2(a) and Fig. 2(b), represents SC for BCD and BSD, respectively, as a function of Eve's distance for different values of the transmitted bandwidth (BW). The distance of the authentic receiver is equal to 10 μm and 150 μm for BCD and BSD respectively. Though, the values of both Eve's and Bob's radius is 10 nm. Irrespective of biological structures, as the value of Eve's distance increases the value of SC increases. Also, as the value of BW is increased for given value of Eve's distance, SC again increases irrespective of biological structures. Though, the nature of the curve ensemble with each other but the magnitude of the SC is more in case of BCD than in case of BSD. This is justified, as apart from different parameters in two deployments, the distance of the

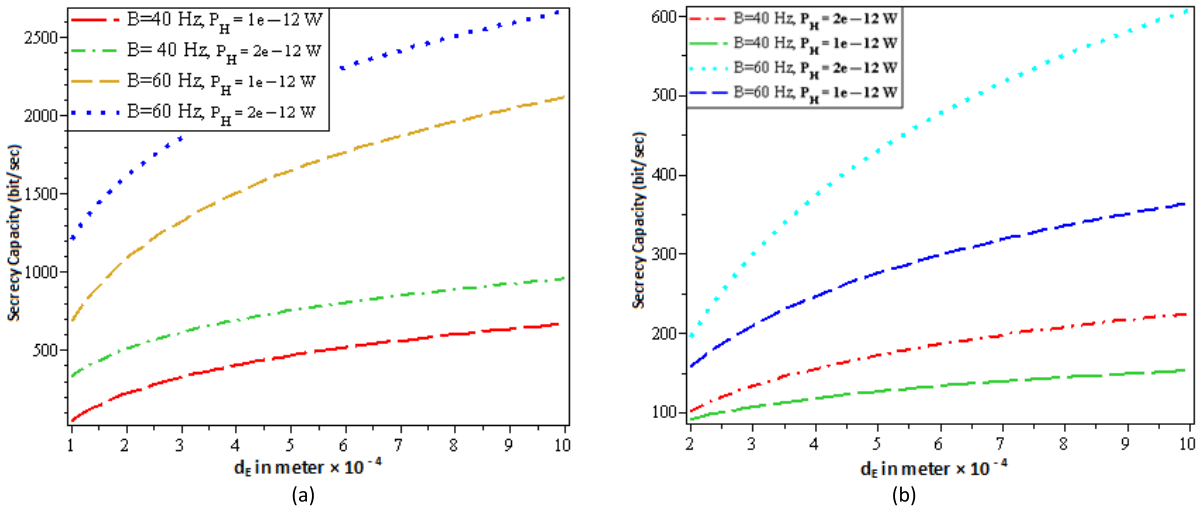

FIGURE 4. The response of Eve's distance over secrecy capacity for different values of transmit power and BW under (a) BCD and (b) BSD.

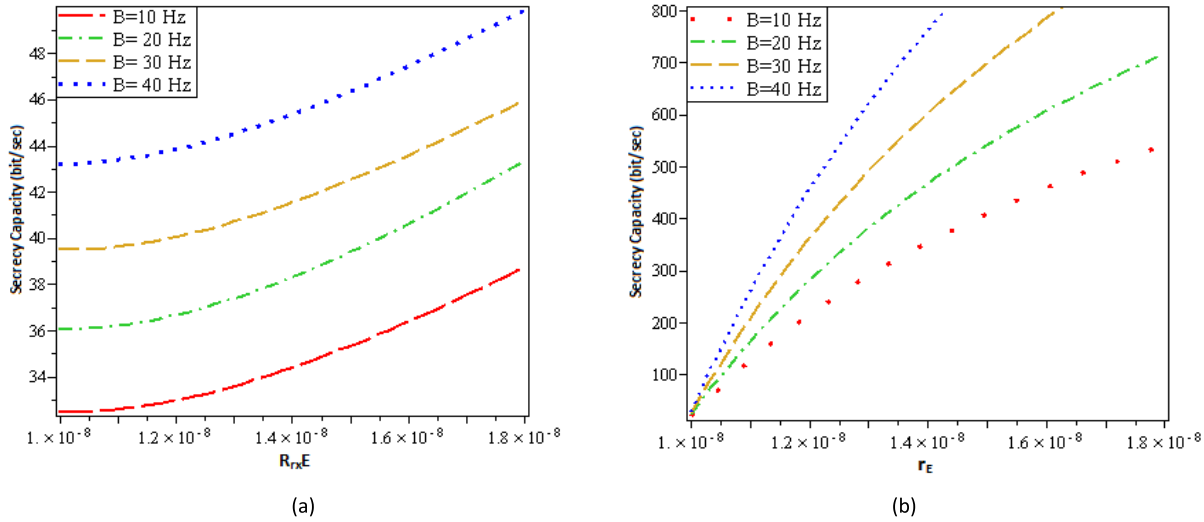

FIGURE 5. The response of Eve's radius over secrecy capacity for different values of BW and transmit power equal to 10^{-12} W under (a) BCD and (b) BSD.

authentic receiver in case of BCD is much lesser than that in case of BSD. In particular, SC is more than 3500 bit/Sec and around 550 bit/Sec for BCD and BSD respectively for BW equal to 10 Hz and Eve's distance equal to 10×10^{-4} m. Also, as the BW is increased from 10 Hz to 40 Hz the SC is more than 6000 bit/Sec and around 1300 bit/Sec for BCD and BSD respectively for same values of eve distance. So, it can be concluded that for given set of respective physical parameters, the SC of BCD is always much more than that of the BSD.

Fig. 3(a) and Fig. 3(b) represents SC of BCD and BSD respectively, as a function of Eve's distance for different values of the transmitted power for BW of 10 Hz. Again, distance of the authentic receiver is equal to 10 μm and 150 μm for BCD and BSD respectively, whereas Eve'/ Bob's radius is 10 nm in either case. Once again, it is observed that as the value of transmitted power increases the value of SC increases. It is observed that for given set of respective parameters and distance of authentic receivers in two deployments, SC of BCD is always much more than that of the BSD.

Fig. 4(a) and Fig. 4(b) represents the SC as a function of Eve's distance for BCD and BSD, respectively for different values of both the BW and transmit power. In both the cases, Eve's/Bob's radius is taken as 10 nm. However, distance of the authentic receiver is equal to 10 μm and 150 μm for BCD and BSD structure respectively. Fig. 4a and Fig. 4b represent combined effect of the parameters shown Fig. 2 and Fig. 3 respectively. However, the observations made with Fig. 4(a) and Fig. 4(b) are same as drawn from Fig. 2 and Fig. 3, respectively.

Fig. 5(a) and Fig. 5(b) represents SC for BCD and BSD respectively, as a function of Eve's radius for different values

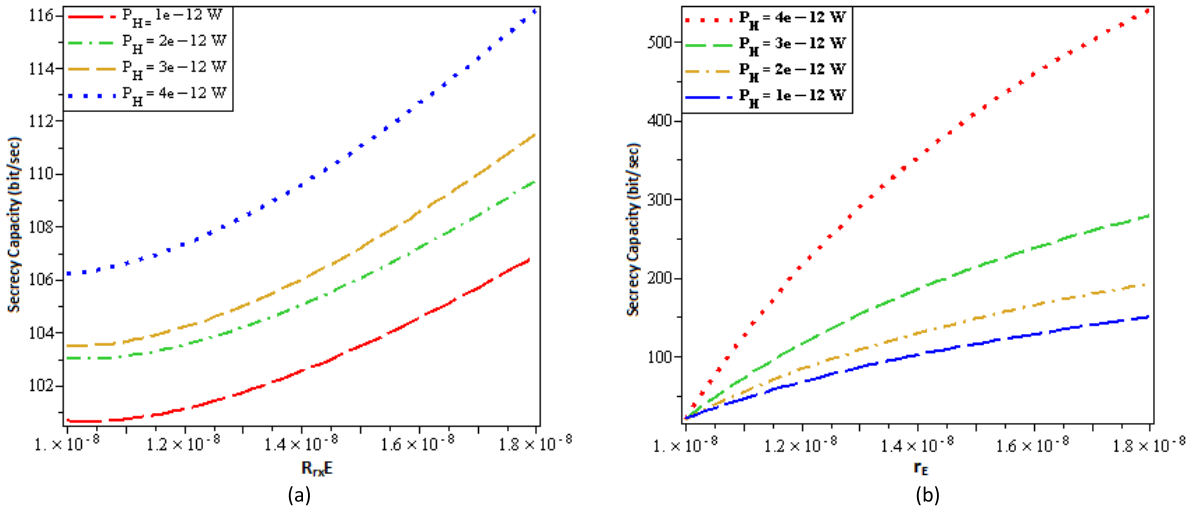

FIGURE 6. The response of Eve's radius over secrecy capacity for different values of transmit power and BW equal to 10 Hz under (a) BCD and (b) BSD.

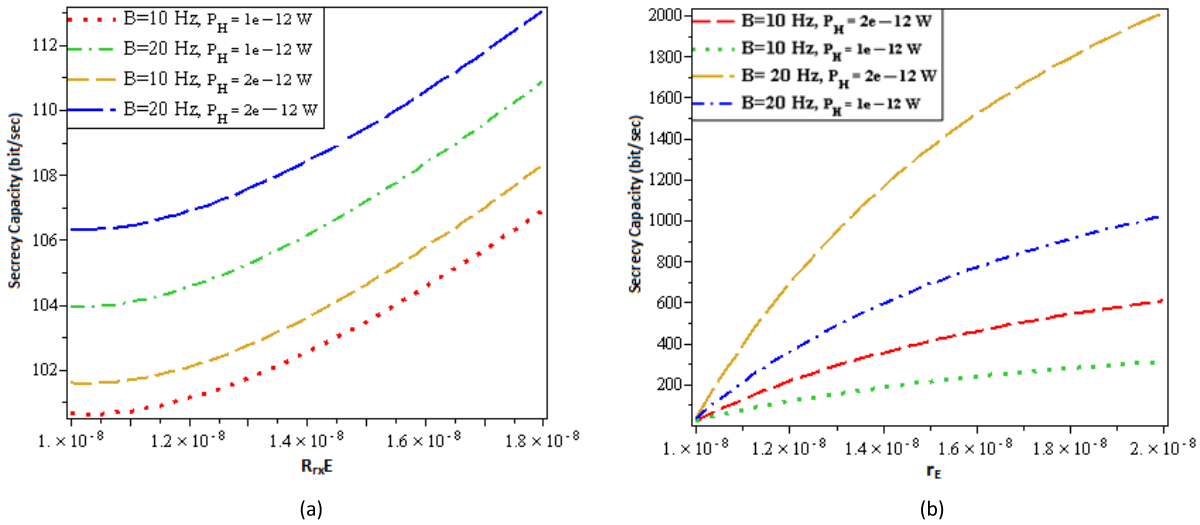

FIGURE 7. The response of Eve's radius over secrecy capacity for different values of transmit power and BW under (a) BCD and (b) BSD.

of the transmitted BW for radius of Bob's equal to 10nm. The distance of the authentic receiver is equal to 10 μm and 150 μm for BCD and BSD respectively. Although the distance of Eve is 15 μm and 1500 μm for BCD and BSD respectively. Irrespective of biological structures, as the value of Eve's radius increases the value of SC increases. Also, as the value of BW is increased from 10 Hz to 40 Hz for given value of Eve's radius, SC again increases irrespective of biological structures. Most important observation drawn from Fig. 5(a) and Fig. 5(b) is that for same values of the distance of the authentic receiver (10 μm and 150 μm for BCD and BSD respectively, which was taken for Fig. 2(a) and Fig. 2(b) to Fig. 4(a) and Fig. 4(b)) if the value of Eve's distance is taken as 15 μm and 1500 μm for BCD and BSD respectively, then the recorded values of SC is more in BSD scheme than in BCD scheme. This means that irrespective of the deployment more is the Eve's from the transmitter lesser is the chance of tapping of the information and hence, higher is the values of SC.

Fig. 6(a) and Fig. 6(b) represents SC for BCD and BSD as a function of Eve's radius for different values of the transmitted power. The values of all the parameters, like radius of Bob's, Eve's distance, and the distance of the authentic receiver for BCD and BSD are same as Fig. 5(a) and Fig. 5(b). It is observed that SC increases with an increase in the value of transmitted power. Also, it is observed that for respective set of the parameter's SC of BSD (with Eve's distance of 1500 μm) is always much more than that of the BCD (with Eve's distance of 15 μm). Fig. 7(a) and Fig. 7(b) represent combined effects of the parameters shown Fig. 5 and Fig. 6 respectively, showing similar observations as made with Fig. 5 and Fig. 6. However, irrespective of all the param-

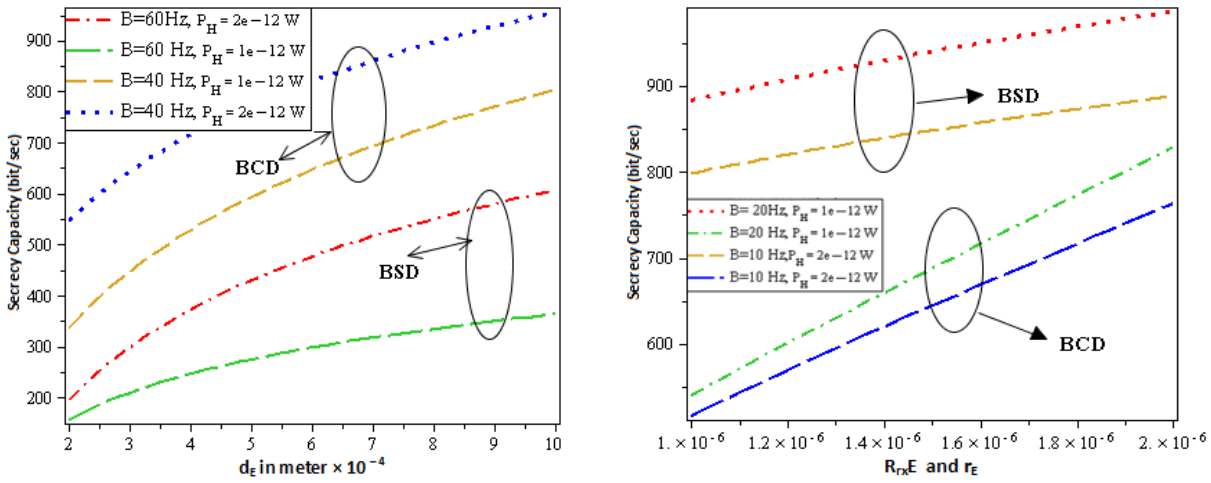

FIGURE 8. The secrecy capacity under BCD and BSD for different values of transmit power and BW as a function of (a) Eve's distance and (b) Eve's radius.

eters BSD has much more SC than BCD as Eve's is far apart in the case of BSD as compared to that of the BCD scheme.

Fig. 8(a) represents comparisons of SC under BCD and BSD schemes as a function of Eve's distance for different values of BW and transmitted power. In case of BCD distance of the authentic receiver and Eve's/Bob's radius is equal to 10 μm and 10 nm respectively. Although the distance of the authentic receiver and Eve's/Bob's radius is equal to 150 μm and 10 nm respectively in case of BSD. As in case of BCD authentic receiver is placed nearer to transmitter (10 μm) compared to that in case of BSD (150 μm). Therefore, irrespective of transmitted power (be it more or less) and even at lesser BW of 40 Hz (compared to 60 Hz), BCD outperform over BSD.

Finally, Fig. 8(b) represents comparisons of SC under BCD and BSD schemes as a function of Eve's radius for different values of BW and transmitted power. In case of BCD, distance of the authentic receiver, Eve's distance and Bob's radius are 10 μm, 150 μm and 10 nm respectively. Whereas, distance of the authentic receiver, distance of Eve and Bob's radius are 150 μm, 1500 μm and 10 nm respectively, in the case of BSD. The value of the authentic receiver and Eve's distance under BSD scheme is more by a factor of 15 and 10, respectively, compared to those under the BCD scheme that results in a very high value of SC under BSD for the same values of BW and transmitted power.

VI. CONCLUSION

Closed-form expressions of the information capacity for the DMC system have been presented under BCD and BSD schemes. The proposed expressions of information capacity have been further employed to derive the expressions of secrecy capacities under the BCD and BSD schemes. The effect of Eve's distance, Eve's radius, the distance of authentic receiver, transmitted power, and BW on the secrecy capacity have been presented under both (BCD and BSD) schemes. It has been observed that irrespective of the deployments, be it BCD or be it BSD, an increase in either of Eve's distance or Eve's radius results in an increase in the value of secrecy capacity. Further, for out of BCD and BSD schemes, an increase in the signal BW and/or transmitted power causes an increase in the secrecy capacity. Also, if the distance of the authentic receiver under the BSD is kept more than that of the BCD by a factor of 15, then the secrecy capacity under BCD is much higher than that of BSD, irrespective of transmitted power (be it more or less) and even at the lesser value of bandwidth. However, if the value of the authentic receiver and Eve's distance with BSD is kept more than that of BCD by a factor of 15 and 10, respectively, then secrecy capacity under BSD is much higher than that of BCD for the same values of bandwidth and transmitted power. It is believed that the proposed analysis is useful for the development of future complex but secured DMC systems under different deployment of biological tissues. To study the effect of different impairments of DMC channels, such as fading and interference on the system performance under proposed deployments, is an open challenge for the future.

APPENDIX A
DERIVATION OF EQ. (9)

$$H(X|\rho) = -\frac{1}{\mathrm{W}}\int_{\mathrm{w}} |C(f)|^2 \mathrm{df}. \tag{A1}$$

Now, substituting value from Eq. (3) into Eq. (A1). We will get:

$$H(X|\rho) = -\frac{1}{\mathrm{W}}\int_{\mathrm{w}} \log_2 \left| \frac{\mathrm{J}_0(\lambda_{\mathrm{k}}\mathrm{r})\, \mathrm{e}^{\lambda_{\mathrm{k}}{}^2 \mathrm{D} t_0}}{\sqrt{\left(\lambda_{\mathrm{k}}{}^2 \mathrm{D}\right)^2 + \omega^2}} \right|^2 \mathrm{df}. \tag{A2}$$

But we have, $w = 2\pi f$. So, Eq. (A2) is simplified as:

$$H\left(X|\rho\right) = -\frac{1}{\mathrm{W}}\int_{\mathrm{w}} \log_2 \left| \frac{\mathrm{J}_0\left(\lambda_{\mathrm{k}}\mathrm{r}\right) \mathrm{e}^{\lambda_{\mathrm{k}}{}^2\mathrm{Dt}_0}}{\sqrt{\left(\lambda_{\mathrm{k}}{}^2\right)^2 + 4\pi^2\mathrm{f}^2}} \right| \mathrm{df}\,. \quad \text{(A3)}$$

Eq. (A3) yields:

$$\begin{aligned} H\left(X|\rho\right) = {} & \frac{1}{\mathrm{W}}\log\left(\lambda_{\mathrm{k}}{}^2\mathrm{D}\right)^2 \\ & + \sum_{\mathrm{i}=1}^{\infty}\left(\frac{2.\pi}{\lambda_{\mathrm{k}}{}^2.\mathrm{D}}\right)^{2\mathrm{i}} . \frac{(-1)^{\mathrm{i}+1}}{(2\mathrm{i}+1)\,\mathrm{i}}\left(\frac{\mathrm{W}}{2\pi}\right)^{2\mathrm{i}+1} \\ & - log\left(2\right) - 2log_2\left(J_0\left(\lambda_k r\right).e^{\lambda_k{}^2.Dt_0}\right). \quad \text{(A4)} \end{aligned}$$

APPENDIX B
DERIVATION OF EQ. (11)

The average particle distribution is given as:

$$\overline{\rho} = E\left[n_t\right]\left(C(f)\right)|_{f=0} \quad \text{(B1)}$$

$$\mathrm{C}_{\mathrm{sph}}\left(\mathrm{f}\right)\big|_{f=0} = \frac{\mathrm{J}_0(\lambda_{\mathrm{k}}r)\mathrm{e}^{\lambda_{\mathrm{k}}{}^2\mathrm{D}(\mathrm{t}-\mathrm{t}_0)}}{\lambda_{\mathrm{k}}{}^2\mathrm{D}}. \quad \text{(B2)}$$

$$\overline{\rho} = E\left[n_t\right]\frac{\mathrm{J}_0(\lambda_{\mathrm{k}}r)\mathrm{e}^{\lambda_{\mathrm{k}}{}^2\mathrm{D}(\mathrm{t}-\mathrm{t}_0)}}{\lambda_{\mathrm{k}}{}^2\mathrm{D}}. \quad \text{(B3)}$$

Also,

$$\begin{aligned} \mathrm{H}\left(\rho|\mathrm{Y}\right) \cong \mathrm{H}\left(\rho\,|\mathrm{E}|\,\mathrm{Y}\right) = {} & \mathrm{E}\left[\mathrm{Y}\right] + \ln\left(2\mathrm{W}\tau_p\right) + \ln\left(\Gamma\left(\mathrm{E}\left[\mathrm{Y}\right]\right)\right) \\ & + (1 - \mathrm{E}[\mathrm{Y}])\psi(\mathrm{E}[\mathrm{Y}]). \quad \text{(B4)} \end{aligned}$$

where, E[Y] is defined as:

$$E[Y] = \frac{2\pi E\left[n_t\right] R_{V_R}}{3}\frac{\mathrm{J}_0(\lambda_{\mathrm{k}}r)\mathrm{e}^{\lambda_{\mathrm{k}}{}^2\mathrm{D}(\mathrm{t}-\mathrm{t}_0)}}{\mathrm{W}\lambda_{\mathrm{k}}{}^2}. \quad \text{(B5)}$$

Finally,

$$\begin{aligned} H(\rho|Y) = {} & \frac{2\pi}{3}\frac{\mathrm{E}\left[n_t\right]\mathrm{R}_{\mathrm{VR}}\mathrm{J}_0(\lambda_{\mathrm{k}}r)\mathrm{e}^{\lambda_{\mathrm{k}}{}^2\mathrm{D}(\mathrm{t}-\mathrm{t}_0)}}{\mathrm{W}\lambda_{\mathrm{k}}{}^2} + \ln\left(2\mathrm{W}\tau_{\mathrm{p}}\right) \\ & + ln\left(\Gamma\left(\frac{2\pi}{3}\frac{\mathrm{E}\left[n_t\right]\mathrm{R}_{\mathrm{VR}}\mathrm{J}_0(\lambda_{\mathrm{k}}r)\mathrm{e}^{\lambda_{\mathrm{k}}{}^2\mathrm{D}(\mathrm{t}-\mathrm{t}_0)}}{\mathrm{W}\lambda_{\mathrm{k}}{}^2}\right)\right) \\ & + \left(1 - \frac{2\pi}{3}\frac{\mathrm{E}\left[n_t\right]\mathrm{R}_{\mathrm{VR}}\mathrm{J}_0(\lambda_{\mathrm{k}}r)\mathrm{e}^{\lambda_{\mathrm{k}}{}^2\mathrm{D}(\mathrm{t}-\mathrm{t}_0)}}{\mathrm{W}\lambda_{\mathrm{k}}{}^2}\right) \\ & \times \psi\left(\frac{2\pi}{3}\frac{\mathrm{E}\left[n_t\right]\mathrm{R}_{\mathrm{VR}}\mathrm{J}_0(\lambda_{\mathrm{k}}r)\mathrm{e}^{\lambda_{\mathrm{k}}{}^2\mathrm{D}(\mathrm{t}-\mathrm{t}_0)}}{\mathrm{W}\lambda_{\mathrm{k}}{}^2}\right). \quad \text{(B6)} \end{aligned}$$

APPENDIX C
DERIVATION OF EQ. (14)

Substituting value from Eq. (5) into Eq. (A1) we will get, (C1), as shown at the bottom of the page. But we have, $w = 2\pi f$. So, Eq. (C1) is simplified as:

$$\begin{aligned} H\left(X|\rho\right) = {} & -\frac{1}{\mathrm{W}}\int_{\mathrm{w}} \log_2 \\ & \times \left(\frac{J_0\left(\lambda_{0m}\rho_{tx}\right)J_0\left(\lambda_{0m}\rho\right)}{2\pi N_{0m}}\frac{\mathrm{e}^{-\left(D\mathrm{d}^2+k_d+\gamma_{0m}{}^2\right)t_0}}{\sqrt{\gamma_{0m}{}^4 + 4\pi^2 f^2}}\right)\mathrm{df}. \end{aligned} \quad \text{(C2)}$$

Eq. (C2) yields:

$$\begin{aligned} H\left(X|\rho\right) = {} & \frac{1}{\mathrm{W}}\log\left(\gamma_{0m}{}^2\right)^2 \\ & + \sum_{\mathrm{i}=1}^{\infty}\left(\frac{2.\pi}{\gamma_{0m}{}^2}\right)^{2\mathrm{i}} . \frac{(-1)^{\mathrm{i}+1}}{(2\mathrm{i}+1)\,\mathrm{i}}\left(\frac{\mathrm{W}}{2\pi}\right)^{2\mathrm{i}+1} \\ & - \log\left(2\right) - 2\log_2 \\ & \times \left(\frac{J_0\left(\lambda_{0m}\rho_{tx}\right)J_0\left(\lambda_{0m}\rho\right)}{2\pi N_{0m}}\mathrm{e}^{-\left(D\mathrm{d}^2+k_d+\gamma_{0m}{}^2\right)t_0}\right). \end{aligned} \quad \text{(C3)}$$

Further, utilizing CGF of the cylindrical environment from Eq. (5) and Eq. (C3), $H(\rho)$ can be given by

$$\begin{aligned} H\left(\rho\right) = {} & \mathrm{H}\left(\mathrm{X}\right) + \mathrm{H}\left(\rho|X\right) - \mathrm{H}\left(X \mid \rho\right) \\ = {} & 2\mathrm{W}.\mathrm{H}\left(\eta_{\mathrm{t}}\right) - \frac{1}{\mathrm{W}}\log\left(\gamma_{0\mathrm{m}}{}^2\right)^2 \\ & - \sum_{\mathrm{i}=1}^{\infty}\left(\frac{2\pi}{\lambda_{\mathrm{k}}{}^2.\mathrm{D}}\right)^{2\mathrm{i}} . \frac{(-1)^{\mathrm{i}+1}}{(2\mathrm{i}+1)\,\mathrm{i}} . \left(\frac{\mathrm{W}}{2\pi}\right)^{2\mathrm{i}+1} \\ & + \log\left(2\right) + 2\log_2 \\ & \times \left(\frac{J_0\left(\lambda_{0m}\rho_{tx}\right)J_0\left(\lambda_{0m}\rho\right)}{2\pi N_{0m}}\mathrm{e}^{-\left(D\mathrm{d}^2+k_d+\gamma_{0m}{}^2\right)t_0}\right). \end{aligned} \quad \text{(C4)}$$

APPENDIX D
DERIVATION OF EQ. (15)

Here,

$$\begin{aligned} \mathrm{C}_{\mathrm{cyl}}\left(\mathrm{f}\right)\big|_{f=0} = {} & \frac{\mathrm{e}^{\left(-Dd^2-k_d-jdv-\gamma_{0m}{}^2\right)(\mathrm{t}-\mathrm{t}_0)}}{2\pi\,\gamma_{0m}{}^2} \\ & \times \frac{J_0\left(\lambda_{0m}\rho_{tx}\right)J_0\left(\lambda_{0m}\rho\right)}{N_{0m}}. \end{aligned} \quad \text{(D1)}$$

Thus, putting Eqn. (D1) into (B1) we get

$$\begin{aligned} \overline{\rho} = {} & E\left[n_t\right]\frac{\mathrm{e}^{\left(-D\mathrm{d}^2-k_d-j\mathrm{d}v-\gamma_{0m}{}^2\right)(\mathrm{t}-\mathrm{t}_0)}}{2\pi\,\gamma_{0m}{}^2} \\ & \times \frac{J_0\left(\lambda_{0m}\rho_{tx}\right)J_0\left(\lambda_{0m}\rho\right)}{N_{0m}}. \end{aligned} \quad \text{(D2)}$$

Also, E[Y] is defined as:

$$\begin{aligned} E\left[Y\right] = {} & \frac{DR_{rx}E\left[n_t\right]}{3W\gamma_{0m}{}^2}\frac{J_0\left(\lambda_{0m}\rho_{tx}\right)J_0\left(\lambda_{0m}\rho\right)}{N_{0m}} \\ & \times \mathrm{e}^{\left(-D\mathrm{d}^2-k_d-j\mathrm{d}v-\gamma_{0m}{}^2\right)(\mathrm{t}-\mathrm{t}_0)}. \end{aligned} \quad \text{(D3)}$$

$$H\left(X|\rho\right) = -\frac{1}{\mathrm{W}}\int_{\mathrm{w}} \left| \frac{\mathrm{e}^{\left(-Dd^2-k_d-j\mathrm{d}v\right)(\mathrm{t}-\mathrm{t}_0)}}{2\pi}\frac{J_0\left(\lambda_{0m}\rho_{tx}\right)J_0\left(\lambda_{0m}\rho\right)}{N_{0m}}\frac{e^{-\gamma_{0m}{}^2\mathrm{t}_0}}{\gamma_{0m}{}^2 + j\omega} \right|^2 \mathrm{df}. \quad \text{(C1)}$$

Finally, from Eqn. (B4)

$$\begin{aligned}
\mathrm{H}(\rho|Y) = & \frac{DR_{rx}E\left[n_t\right]}{3W{\gamma_{0m}}^2}\frac{J_0\left(\lambda_{0m}\rho_{tx}\right)J_0\left(\lambda_{0m}\rho\right)}{N_{0m}} \\
& \times \mathrm{e}^{\left(-D\mathrm{d}^2-k_d-j\mathrm{d}v-{\gamma_{0m}}^2\right)(\mathrm{t}-\mathrm{t}_0)} + \ln\left(2W\tau_{\mathrm{p}}\right) \\
& + ln\left(\Gamma\left(\frac{DR_{rx}E\left[n_t\right]}{3W{\gamma_{0m}}^2}\frac{J_0\left(\lambda_{0m}\rho_{tx}\right)J_0\left(\lambda_{0m}\rho\right)}{N_{0m}}\right.\right. \\
& \left.\left.\times\ \mathrm{e}^{\left(-D\mathrm{d}^2-k_d-j\mathrm{d}v-{\gamma_{0m}}^2\right)(\mathrm{t}-\mathrm{t}_0)}\right)\right) \\
& + \left(1-\frac{DR_{rx}E\left[n_t\right]}{3W{\gamma_{0m}}^2}\frac{J_0\left(\lambda_{0m}\rho_{tx}\right)J_0\left(\lambda_{0m}\rho\right)}{N_{0m}}\right. \\
& \left.\times\ \mathrm{e}^{\left(-D\mathrm{d}^2-k_d-j\mathrm{d}v-{\gamma_{0m}}^2\right)(\mathrm{t}-\mathrm{t}_0)}\right) \\
& \times \psi\left(\frac{DR_{rx}E\left[n_t\right]}{3W{\gamma_{0m}}^2}\frac{J_0\left(\lambda_{0m}\rho_{tx}\right)J_0\left(\lambda_{0m}\rho\right)}{N_{0m}}\right. \\
& \left.\times\ \mathrm{e}^{\left(-D\mathrm{d}^2-k_d-j\mathrm{d}v-{\gamma_{0m}}^2\right)(\mathrm{t}-\mathrm{t}_0)}\right). \qquad \text{(D4)}
\end{aligned}$$

ACKNOWLEDGMENT

An earlier version of this paper was presented in part at the 1st ACM International Workshop on Nanoscale Computing, Communication, and Applications NanoCoCoA-2020 [DOI: 10.1145/3416006.3431277].

REFERENCES

[1] P.-C. Yeh, K. C. Chen, Y. C. Lee, L. S. Meng, P. J. Shih, P. Y. Ko, W. A. Lin, and C. H. Lee, "A new frontier of wireless communication theory: Diffusion-based molecular communications," *IEEE Wireless Commun.*, vol. 19, no. 5, pp. 28–35, Oct. 2012.

[2] N. Farsad, H. B. Yilmaz, A. Eckford, C. B. Chae, and W. Guo, "A comprehensive survey of recent advancements in molecular communication," *IEEE Commun. Surveys Tuts.*, vol. 18, no. 3, pp. 1887–1919, 3rd Quart., 2016.

[3] M. Turan, M. S. Kuran, H. B. Yilmaz, I. Demirkol, and T. Tugcu, "Channel model of molecular communication via diffusion in a vessel-like environment considering a partially covering receiver," in *Proc. IEEE Int. Black Sea Conf. Commun. Netw. (BlackSeaCom)*, Aug. 2018, pp. 1–5.

[4] Y. Chahibi, M. Pierobon, S. O. Song, and I. F. Akyildiz, "A molecular communication system model for particulate drug delivery systems," *IEEE Trans. Biomed. Eng.*, vol. 60, no. 12, pp. 3468–3483, Dec. 2013.

[5] N. Farsad, A. W. Eckford, S. Hiyama, and Y. Moritani, "On-chip molecular communication: Analysis and design," *IEEE Trans. Nanobiosci.*, vol. 11, no. 3, pp. 304–314, Sep. 2012.

[6] Y. Moritani, S. Hiyama, and T. Suda, "Molecular communication for health care applications," in *Proc. 4th Annu. IEEE Int. Conf. Pervasive Comput. Commun. Workshops (PERCOMW)*, Mar. 2006, p. 5.

[7] L. P. Giné and I. F. Akyildiz, "Molecular communication options for long range nanonetworks," *Comput. Netw.*, vol. 53, no. 16, pp. 2753–2766, 2009.

[8] A. O. Bicen and I. F. Akyildiz, "Molecular transport in microfluidic channels for flow-induced molecular communication," in *Proc. IEEE Int. Conf. Commun. Workshops (ICC)*, Jun. 2013, pp. 766–770.

[9] M. Zoofaghari and H. Arjmandi, "Diffusive molecular communication in biological cylindrical environment," *IEEE Trans. Nanobiosci.*, vol. 18, no. 1, pp. 74–83, Jan. 2019.

[10] R. L. Fournier, *Basic Transport Phenomena in Biomedical Engineering*. Boca Raton, FL, USA: CRC Press, Aug. 2017.

[11] H. Arjmandi, M. Zoofaghari, and A. Noel, "Diffusive molecular communication in a biological spherical environment with partially absorbing boundary," *IEEE Trans. Commun.*, vol. 67, no. 10, pp. 6858–6867, Oct. 2019.

[12] F. Walsh, S. Balasubramaniam, D. Botvich, and W. Donnelly, "Synthetic protocols for nano sensor transmitting platforms using enzyme and DNA based computing," *Nano Commun. Netw.*, vol. 1, no. 1, pp. 50–62, 2010.

[13] R. Waehler, S. J. Russell, and D. T. Curiel, "Engineering targeted viral vectors for gene therapy," *Nature Rev. Genet.*, vol. 8, no. 8, pp. 573–587, Aug. 2007.

[14] J. Tan, A. Thomas, and Y. Liu, "Influence of red blood cells on nanoparticle targeted delivery in microcirculation," *Soft Matter*, vol. 8, no. 6, pp. 1934–1946, 2012.

[15] L. Felicetti, M. Femminella, and G. Reali, "Simulation of molecular signaling in blood vessels: Software design and application to atherogenesis," *Nano Commun. Netw.*, vol. 4, no. 3, pp. 98–119, Sep. 2013.

[16] P. Birner, G. Prager, and B. Streubel, "Molecular pathology of cancer: How to communicate with disease," *ESMO Open*, vol. 1, no. 5, 2016, Art. no. e000085.

[17] R. Bayraktar, K. Van Roosbroeck, and G. A. Calin, "Cell-to-cell communication: MicroRNAs as hormones," *Mol. Oncol.*, vol. 11, no. 12, pp. 1673–1686, Dec. 2017.

[18] P. Mr, "Genetic mechanisms an open thermodynamic system of an organism in norm and pathology," *J. Mol. Genetic Med.*, vol. 12, no. 2, pp. 0862–1747, 2018.

[19] D. Oron, E. Papagiakoumou, F. Anselmi, and V. Emiliani, "Two-photon optogenetics," in *Progress in Brain Research*, vol. 196. Amsterdam, The Netherlands: Elsevier, Jan. 2012, pp. 119–143, doi: 10.1016/b978-0-444-59426-6.00007-0.

[20] S. A. Wirdatmadja, M. T. Barros, Y. Koucheryavy, J. M. Jornet, and S. Balasubramaniam, "Wireless optogenetic nanonetworks for brain stimulation: Device model and charging protocols," *IEEE Trans. Nanobiosci.*, vol. 16, no. 8, pp. 859–872, Dec. 2017.

[21] M. S. Kuran, H. B. Yilmaz, and T. Tugcu, "A tunnel-based approach for signal shaping in molecular communication," in *Proc. IEEE Int. Conf. Commun. Workshops (ICC)*, Jun. 2013, pp. 776–781.

[22] W. Wicke, T. Schwering, A. Ahmadzadeh, V. Jamali, A. Noel, and R. Schober, "Modeling duct flow for molecular communication," in *Proc. IEEE Global Commun. Conf. (GLOBECOM)*, Dec. 2018, pp. 206–212.

[23] M. M. Al-Zu'bi and A. S. Mohan, "Modeling of ligand-receptor protein interaction in biodegradable spherical bounded biological microenvironments," *IEEE Access*, vol. 6, pp. 25007–25018, 2018.

[24] F. Dinç, B. C. Akdeniz, A. E. Pusane, and T. Tugcu, "Impulse response of the molecular diffusion channel with a spherical absorbing receiver and a spherical reflective boundary," *IEEE Trans. Mol., Biol. Multi-Scale Commun.*, vol. 4, no. 2, pp. 118–122, Jun. 2018.

[25] X. Bao, Y. Zhu, and W. Zhang, "Channel characteristics for molecular communication via diffusion with a spherical boundary," *IEEE Wireless Commun. Lett.*, vol. 8, no. 3, pp. 957–960, Jun. 2019.

[26] G. Alfano and D. Miorandi, "On information transmission among nanomachines," in *Proc. 1st Int. Conf. Nano-Netw. Workshops*, Sep. 2006, pp. 1–5.

[27] A. Einolghozati, M. Sardari, A. Beirami, and F. Fekri, "Capacity of discrete molecular diffusion channels," in *Proc. IEEE Int. Symp. Inf. Theory*, Jul. 2011, pp. 723–727.

[28] M. Pierobon and I. F. Akyildiz, "Capacity of a diffusion-based molecular communication system with channel memory and molecular noise," *IEEE Trans. Inf. Theory*, vol. 59, no. 2, pp. 942–954, Feb. 2013.

[29] L. Mucchi, A. Martinelli, S. Jayousi, S. Caputo, and M. Pierobon, "Secrecy capacity and secure distance for diffusion-based molecular communication systems," *IEEE Access*, vol. 7, pp. 110687–110697, 2019.

[30] S. Singh, P. P. Galgotias, S. P. Singh, and M. Lakshmanan, "Information capacity analysis of DMC under spherical biological system," in *Proc. 7th Int. Conf. Signal Process. Integr. Netw. (SPIN)*, Feb. 2020, pp. 946–949.

[31] S. P. Singh, S. Yadav, and S. Mishra, "Secrecy capacity of diffusive molecular communication under biological spherical environment," in *Proc. 1st ACM Int. Workshop Nanoscale Comput., Commun., Appl.*, Nov. 2020, pp. 33–38.

[32] D. S. Lemons, A. Gythiel, and P. Langevin, "Sur la théorie du mouvement brownien [On the theory of Brownian motion]," *CR Acad. Sci. (Paris)*, vol. 146, pp. 530–533, Mar. 1908.

[33] T. M. Cover and J. A. Thomas, *Elements of Information Theory*, 2nd ed. New York, NY, USA: Wiley, 2006.

S. PRATAP SINGH (Member, IEEE) is currently working as a Professor with the Department of Electronics and Communication Engineering, GCET, Greater Noida, India. He has more than 18 years of experience in teaching and research. The goal of his life is to implements MNC and/or EMNC system, the application of which ranges from military to medical, information communication to bio-informatics and industry to environment, in short, almost in every aspect of life. He has published several research papers in reputed journals of IEEE, Elsevier, Springer, Wiley, and Taylor's & Francis apart from many more Scopus indexed research papers through different international conferences. He has also published two IPR from India and one book chapter ''Multimedia Nano Communication for Healthcare: Noise Analysis.'' His current research interests include modeling, analysis, and mitigation of fading, interference and noise in wireless communication and nano communication, which includes electromagnetic nano communication (EMNC) using terahertz band and molecular nano communication (MNC) using molecules via gaseous or aqueous medium. He is a fellow of IETE, India.

SUMAN YADAV received the M.Tech. degree in electronics and communication engineering. She has published her M.Tech. research in ''radioelectronics and communications systems,'' a reputed journal of Springer. She is currently a Ph.D. Scholar at NIT Patna, India. She is also working as an Assistant Professor with the Lloyd Institute of Engineering and Technology, Greater Noida, India. Recently, she has published one invited paper in NanoCoCoA-2020, the 18th ACM Conference on Embedded Networked Sensor Systems SenSys-2020. Also, parts of the work has been presented and get published in reputed international conferences, such as 18th International Symposium on Wireless Personal Multimedia Communications, WPMC-2015, and IEEE UP Section Conference on Electrical Computer and Electronics (UPCON-2015).

RAJNEESH KUMAR SINGH received the M.Tech. degree in computer science from Jamia Hamdard University, New Delhi, India, in 2013. He is currently pursuing the Ph.D. degree in computer science and engineering with Dr. A. P. J. Abdul Kalam University, Lucknow, India. He is currently working as an Assistant Professor at GCET, Greater Noida, India. He has more than 14 years of experience in teaching and research. He has published various research papers in reputed journals of Elsevier, Wiley, and Taylor's & Francis. He has also published several papers in Scopus indexed international conferences of IEEE. His research interests include modeling, analysis, and mitigation of various impairments in nano communication and networks.

VINEET KANSAL studied at the Indian Institute of Technology, Delhi. He is currently working as a Professor with the Institute of Engineering and Technology, Dr. A. P. J. Abdul Kalam Technical University, Lucknow. His research interests include artificial intelligence, machine learning, software engineering, and nano networks. He was awarded appreciation by NPTEL, IIT Kanpur, and the Centre of Continuing Education, IIT Kanpur, for inspiring the faculty members and students of higher technical education to adopt NPTEL online certification courses, for evangelizing it's modus operandi and for conceptualizing online and offline blended faculty training programs addressing pedagogical issues in engineering education in the state of Uttar Pradesh, India.

GHANSHYAM SINGH received the Ph.D. degree in electronics engineering from the Indian Institute of Technology, Banaras Hindu University, Varanasi, India, in 2000. He was associated with the Central Electronics Engineering Research Institute, Pilani, and the Institute for Plasma Research, Gandhinagar, India, as a Research Scientist. He had also worked as an Assistant Professor at the Electronics and Communication Engineering Department, Nirma University of Science and Technology, Ahmedabad, India. He was a Visiting Researcher at Seoul National University, Seoul, South Korea. He has worked as a Professor with the Department of Electronics and Communication Engineering, Jaypee University of Information Technology, Waknaghat, Solan, India. He is currently working as a Professor and the Director of the Centre for Smart Information and Communication Systems, Department of Electrical and Electronics Engineering Sciences, Auckland Park Kingsway Campus, University of Johannesburg, South Africa. He has more than 21 years of teaching and research experience in the area of electromagnetic/microwave engineering, wireless communication, and nanophotonics. He has supervised various M.Tech. and Ph.D. theses. He is the author/coauthor of several books/book chapters published by Springer Nature, Elsevier, Wiley, and IET, and more than 270 scientific papers of the refereed journal and international conferences. His teaching and research interests include RF/microwave engineering, millimeter/THz wave antennas, and its applications in communication and imaging, next generation communication systems (OFDM and cognitive radio), and nanophotonics.